GENERAL INSTRUCTION

- **Authors: Carefully check the page proofs (and coordinate with all authors); additional changes or updates WILL NOT be accepted after the article is published online in its final form. Please check author names and affiliations, funding, as well as the overall article for any errors prior to sending in your author proof corrections. Your article has been peer reviewed, accepted as final, and sent in to IEEE. No text changes have been made to the main part of the article as dictated by the editorial level of service for your publication.**
- **Authors: Please check ALL author names for correct spelling, abbreviations, and order of first and last name in the byline and affiliation footnote.**
- **Authors: We cannot accept new source files as corrections for your article. If possible, please annotate the PDF proof we have sent you with your corrections and upload it via the Author Gateway. Alternatively, you may send us your corrections in list format. You may also upload revised graphics via the Author Gateway.**
- **Authors: Please note that once you click "approve with no changes," the proofing process is now complete and your article will be sent for final publication and printing. Once your article is posted on Xplore, it is considered final and the article of record. No further changes will be allowed at this point so please ensure scrutiny of your final proof.**
- **Authors: Unless invited or otherwise informed, a mandatory Excessive Article Length charges will be incurred if your article is over the page limit set by the society in the Information for Authors.**

QUERIES

Q1. Author: Please provide an abstract of fewer than 250 words.
Q2. Author: Please confirm or add details for any funding or financial support for the research of this article.
Q3. Author: Please provide full page range in Refs. [4], [5], [14], [24], [35], [44], and [66].
Q4. Author: Please provide complete bibliographic details for Refs. [8] and [39].
Q5. Author: Please provide Volume number in Ref. [52].

A Controlled Thermoalgesic Stimulation Device for Exploring Novel Pain Perception Biomarkers

Maider Núñez Ibero, Borja Camino-Pontes, Ibai Diez, Asier Erramuzpe, Endika Martínez Gutiérrez, Sebastiano Stramaglia, Javier Ortiz Álvarez-Cienfuegos, and Jesus M. Cortes

***Abstract*—Objective: To develop a new device useful for identifying physiological markers of pain perception by reading the brain's electrical activity and hemodynamic interactions while applying thermoalgesic stimulation. Methods: We designed a compact prototype that generates well-controlled thermal stimuli using a computer driven Peltier cell while simultaneously capturing electroencephalography (EEG) and photoplethysmography (PPG) signals as the stimuli are varied. The study was performed on 35 healthy subjects (mean age 30.46 years, SD 4.93 years; 20 males, 15 females). To account for the inter-subject variability in the tolerance to thermal pain, we first determined the heat pain threshold (HPT) for each subject, defined as the maximum temperature that the subject can withstand when the Peltier cell gradually increases the temperature. Subsequently, we defined the pain parameters associated with a stimulation temperature equivalent to 90% of the HPT, comparing this to the no-pain state (control) in the absence of thermoalgesic stimulation. Results: Both the one-dimensional and the two-dimensional spectral entropy (SE) obtained from both the EEG and PPG signals differentiated the condition of pain. In particular, the SE for PPG was significantly reduced in association with pain, while the SE for EEG increased slightly. Moreover, significant discrimination occurred within a specific range of frequencies, 26-30 Hz for EEG and about 5-10 Hz for PPG. Conclusion: Hemodynamics, brain dynamics and their interactions can discriminate thermal pain perception. Significance: The possibility of monitoring on-line variations in thermal pain perception using a similar device and algorithms may be of interest to study different pathologies that affect the peripheral nervous system, such as small fiber neuropathies, fibromyalgia or painful diabetic neuropathy.**

***Index Terms*—Thermoalgesic stimulation, heat pain threshold, spectral entropy, pain perception, photoplethysmography, electroencephalography, biopac.**

Manuscript received August 6, 2020; revised March 26, 2021; accepted May 8, 2021. This work was supported in part by the JMC, funded by Ikerbasque: The Basque Foundation for Science, Ministerio Economia, Industria y Competitividad, Spain, and FEDER under Grant DPI2016-79874-R, and in part by the Department of Economic Development and Infrastructure of the Basque Country (Elkartek Program) under Grants KK-2018/00032 and KK-2018/00090. The work of Borja Camino-Pontes was supported by the Department of Education of the Basque Country Predoctoral Program under Grant PRE-2020-1-0187. The work of Asier Erramuzpe was supported in part by the ELSC and in part by the Department of Education of the Basque Country Postdoctoral Program under Grant POS-2019-2-0020). The work of Endika Martínez Gutiérrez was supported by the Department of Education of the Basque Country postdoctoral program under Grant POS-2019-1-0034. *(Maider Núñez Ibero and Borja Camino-Pontes contributed equally to this work and are co-first authors.) (Javier Ortiz Á lvarez-Cienfuegos and Jesus M. Cortes contributed equally to this work and are co-senior authors.) (Corresponding author: Jesus Maria CortesDiaz.)*

Maider Núñez Ibero is with Biomedical Research Doctorate Program, University of the Basque, 48940 Leioa, Spain (e-mail: maidernunezibero@gmail.com).

Borja Camino-Pontes is with Biocruces-Bizkaia Health Research Institute, 48903 Barakaldo, Spain (e-mail: caminopontes@gmail.com).

Ibai Diez is with the Gordon Center for Medical Imaging, Department of Radiology, Massachusetts General Hospital and Harvard Medical School, Boston, MA 02115 USA and with the Athinoula A. Martinos Center for Biomedical Imaging, Massachusetts General Hospital, Harvard Medical School, Boston, MA 02115 USA (e-mail: ibaidiez85@gmail.com).

Asier Erramuzpe is with Biocruces-Bizkaia Health Research Institute, 48903 Barakaldo, Spain, with The Edmond & Lily Safra Center for Brain Sciences, Hebrew University of Jerusalem, Jerusalem, Israel and also with Biomedical Engineering Department, Faculty of Engineering, Mondragon University, Mondragon, Spain (e-mail: asier.erramuzpe@gmail.com).

Endika Martínez Gutiérrez is with the Biocruces-Bizkaia Health Research Institute, 48903 Barakaldo, Spain, with the Dipartamento Interateneo di Fisica, Universita di Bari, and also with the INFN, 70121 Sezione di Bari, Italy (e-mail: emargu92@gmail.com).

Sebastiano Stramaglia is with the Dipartamento Interateneo di Fisica, Universita di Bari, and INFN, 70121 Sezione di Bari, Italy (e-mail: Sebastiano.Stramaglia@ba.infn.it).

Javier Ortiz Álvarez-Cienfuegos is with the Department of Electronic Technology, University of the Basque, 48940 Bilbao, Spain (e-mail: javier.ortiza@ehu.eus).

Jesus M. Cortes is with Biocruces-Bizkaia Health Research Institute, 48903 Barakaldo, Spain, with the IKERBASQUE: The Basque Foundation for Science, Bilbao, Spain, and also with the Department of Cell Biology and Histology, University of the Basque, 48940 Leioa, Spain (e-mail: jesus.m.cortes@gmail.com).

Digital Object Identifier 10.1109/JBHI.2021.3080935

I. Introduction

THE synergy between electronic technology and state-of-the-art instrumentation, together with the incorporation of statistical analysis and data science, provides tremendous possibilities in neuroscience research [1]. Here, following previous works [2]–[4] we have designed a new, compact hardware-device to measure systemic responses of the peripheral nervous system (PNS), such as the perception of pain, by progressively increasing a Peltier cell's temperature in contact with a subjects skin or hand. The device allows simultaneously recording of brain and heart dynamics by measuring electroencephalography (EEG) and photoplethysmography (PPG),[1] respectively.

[1]While the physiological meaning of PPG is unclear as it is affected by multiple mechanisms such as baroreflex sensitivity, blood pressure, and vasodilation/constriction, here in this study, we used this signal as a proxy for the hemodynamic response.

Therefore, our device can be used to quantitatively measure systemic physiological responses to thermal stimulation, allowing the underlying structural and functional changes to be elucidated, and offering an insight into the physiological interactions provoked, the so-called physiolome [5]–[7].

But what exactly is pain perception and how can it be measured? A definition of pain was formulated more than 50 years ago [8]: *Pain is an unpleasant experience that we primarily associate with tissue damage or describe in terms of tissue damage or both*. Since then, multidisciplinary approaches and the emergence of models for chronic pain-related disease have produced substantial advances in our understanding of pain, its assessment and treatment. As such, a more refined definition has been proposed by the International Association for the Study of Pain, whereby: *Pain is an unpleasant sensory and emotional experience associated with actual or potential tissue damage, or described in terms of such damage*. Accordingly, it is now well-accepted that pain encompasses a systemic response that can be detected or perceived over quite different scales and systems.

Here we have asked whether pain perception might be encoded through different physiological signals and we sought to assess their possible interactions. The physiological response to pain has been addressed previously using approaches like near-infrared spectroscopy (fNIRS) [9], laser Evoked Potential (LEPs) [10], EEG [11]–[13] and PPG [14], [15], yet these signals are typically analyzed separately. Moreover, the paradigm to produce painful stimulation relies on human intervention [16] or environmental factors [17], which may compromise the reliability of these results. By contrast, the device we have designed produces well-controlled painful stimulation. Although not yet approved by the Food and Drug Administration (FDA), General Electric Healthcare introduced the Surgical Pleth Index (SPI) to measure the increase in sympathetic activity from the PPG signal in response to painful (nociceptive) stimuli [18]. However, the SPI only works in conjunction with general anesthesia and thus, much of the cortical processing that occurs when a painful stimulus is received is also ignored. Moreover, the precise relationship between the entropy of physiological responses and pain perception remains unclear. Nevertheless, the relationship between variations in entropy following exposure to a nociceptive stimulus has been assessed previously [19], showing an increase in the spatial entropic patterns in response to painful stimuli.

Here we have studied the dynamic physiological interactions that are produced in response to a painful stimulus in an attempt to advance the perception of pain. In contrast to other studies, we have designed and used a device that objectively controls the painful thermal stimulus generated, whilst synchronously recording electrical neuronal activity and some hemodynamic parameters. The main working hypothesis is that by simultaneously monitoring these variables in response to a painful stimulus and comparing them to the basal response, novel aspects of sympathetic excitation and regulation might be revealed in relation to the perception of pain. From the data obtained, we intend to validate the usefulness of our system to evaluate groups of patients with different pathologies associated with abnormalities in the PNS.

II. Methods

A. Hardware

To design and manufacture an electronic device to generate the stimuli, we used OrCAD (version 16.6 Lite) to automate the production of the printed circuit, the board design and photolithography, and for the chemical etching to finally manufacture the boards. Once the circuit boards were designed and manufactured, the electronic components were inserted and soldered onto them at the Electronic Technology laboratory in the Bilbao School of Engineering. Very briefly, the platform is composed by a brand-new thermal stimulus generator and a Biopac (BioPac Systems, Inc, Student Lab MP36), a registered device that captures EEG and PPG signals simultaneously through silver/silver chloride gel type sensors. The thermal stimulus generator is made up of 4 electronic interconnected boards, one for the power supply, and the three following more:

- A temperature controlling board to generate the pulse-width modulation to the power board to regulate the electric current through the Peltier modules.
- A heat-cool selector board to switch between hot and cold generation in Peltier plates, mainly due to a 30 A relay.
- A power board to transfer power to the Peltier plates implemented by a full-bridge N-channel power MOSFET, followed by a LC output filter to smooth the output current.

The Hot-Cold spots of the thermal stimulus generator are regulated using a 120 Watt Peltier module (40x40 mm, TEC1-12710), with internal structure formed by stacked layers of very small cells which assure a smooth homogeneous heat distribution. The module is built on top of a 120 Watt capacity air cooler and covered by a thermal pad (conductivity>4 W/mK, Laird Technologies, 110x100x2.5 mm) on which the hand palm is placed always in the same position.

We used MATLAB (version R2017a, MathWorks Inc., Natick, MA, USA) to create the user interface, connecting it to the hardware device that generates the stimuli, to process the physiological signals, run the spectral entropy (SE) algorithms, present the results and prepare the final images. The BioPac system was configured to read the physiological variables and the data obtained was processed using the AcqKnowledge software (version BSL PRO 3.7), which records, analyses and filters the data in real-time, presenting it as a continuous record, an X-Y chart or a histogram.

B. Participants and Ethical Considerations

The study was carried out on 35 healthy volunteers (20 men; 15 women) recruited at the University of the Basque Country and with a mean age of 30.46 years (SD 4.93 years). For demographic details see Table I. All the participants provided their signed informed consent and the study was approved by the Ethical Committee of the University of the Basque Country (project code 2017/092). The data were acquired according to the guidelines laid down by the University's Ethical Committee and the Ethical Principles for Medical Research Involving Human Subjects set out in the Helsinki Declaration. The inclusion criteria were to be aged between 20 and 40 years-old and to

TABLE I
SEX, AGE, HAND STIMULATED AND HEAT PAIN THRESHOLD (HPT) (°C) FOR ALL PARTICIPANTS (N = 35, 20 MEN;15 WOMEN.)

	Sex	Age	Hand Heated	HPT
Subject 1	M	32	Right	43.23
" 2	F	28	Right	45.02
" 3	M	24	Right	41.23
" 4	F	30	Right	44.12
" 5	M	30	Right	43.00
" 6	M	33	Right	42.75
" 7	M	36	Right	38.80
" 8	M	33	Right	41.89
" 9	F	36	Right	42.13
" 10	F	31	Right	41.60
" 11	F	31	Right	44.42
" 12	M	23	Right	44.03
" 13	F	30	Right	43.47
" 14	M	31	Right	40.98
" 15	F	40	Left	42.82
" 16	F	20	Right	42.60
" 17	M	20	Right	44.67
" 18	M	38	Right	41.22
" 19	M	26	Right	42.32
" 20	F	25	Right	42.49
" 21	F	31	Right	43.07
" 22	M	30	Right	42.89
" 23	M	36	Right	44.10
" 24	M	36	Right	44.23
" 25	M	31	Left	44.10
" 26	M	31	Left	41.52
" 27	F	24	Left	43.10
" 28	F	30	Left	41.35
" 29	M	33	Left	41.56
" 30	F	27	Left	41.84
" 31	M	33	Left	44.10
" 32	M	28	Left	44.3
" 33	F	22	Left	40.95
" 34	M	35	Left	41.83
" 35	F	26	Left	41.91

have provided signed informed consent. The age interval of 20-40 years old was chosen due to two major reasons: 1. To control the effect of age, and therefore eliminating paediatric or old populations. 2. For ethical committee recommendations as this study recruited participants in the university environment, dominating this interval of age. The exclusion criteria were any diagnosed illness, medication use or drug consumption in the month prior to testing, the refusal of the volunteer to participate in the study or the consumption of energetic drinks immediately prior to testing.

C. Capture and Cleaning of Physiological Signals

Before starting the experiments, the subjects were seated near a table with a computer on it, listening to relaxing music so that the experiments commenced in a calm and emotional state. In order to minimize eye-blinking artifacts, all subjects were asked to remain silent with their eyes closed, and to stay still without crossing their legs throughout the experiment. The physiological variables captured were the EEG signals from both cerebral hemispheres and the PPG signals from the contralateral hand to that being heated by the Peltier cell (see Fig. 1(a)).

The EEG signals were obtained through six electrodes situated in accordance with the Electrode Position Modified Combinatorial Nomenclature [20], two on one cerebral hemisphere, another two on the other hemisphere and two more as reference points. The electrodes used were silver/silver chloride gel types. The EEG electrodes were located on the forehead using a bipolar arrangement, measuring the differentiated voltages between the FP1 (Frontal Pole) and AF7 (Anterior Frontal) electrodes in one of the channels, and between the symmetrical FP2 and AF8 points in the second channel. For the reference electrodes, the first channel uses an electrode in the lower front central position, while the second channel uses the upper front central position. A differential distribution was employed with separate but analogous reference points, such that the readings from the left and right hemispheres are largely comparable. The EEG electrode location at the frontal positions guarantees a superior amplitude and integrity of the signals acquired, resulting in a lower impedance of the electrode-skin interface. Moreover, the prefrontal locations of the EEG might modulate the pain-related autonomic response [21].

The PPG signal was acquired by attaching a transducer to the tip of the index finger, consisting of a matched infrared emitter and a photodiode detector that transmits the changes in infrared reflectance resulting from the variation in blood flow. When the PPG transducer is placed on the skin, close to the capillaries, the reflectance of the infrared light from the emitter to the detector will change in accordance with the capillary blood volume, enabling the blood volume pulse waveform to be recorded. It is important to note that the PPG signal is an efficient and interesting alternative to measure heartbeat intervals, since it is simpler than the electrocardiogram while achieving a precise measurement for heart rate variability [22].

All the signals were filtered with a 38.5 Hz Low Pass Notch Filter incorporated into the series amplifier modules of BioPac, thereby eliminating the 50 Hz mains interference. Two differentiated signals (FP1 minus AF7 and FP2 minus AF8) were obtained and filtered using a recent data-driven algorithm that removes ocular and muscle artifacts from the single-channel data, referred as the surrogate-based artifact removal (SuBAR) method [23]. Although the full details are given elsewhere [23], the algorithm briefly performs: 1. Z-score of the data; 2. Maximal Overlap Wavelet Transform (MODWT) of the data, using symlets of order 5 and with 5 levels of decomposition; 3. Removal of artifacts, defined as the values of the wavelet coefficients that are outliers relative to the distribution of the values obtained from the data surrogates (to identify outliers, we considered a 5% significance level and the outlier coefficients were eliminated by substituting their values with the average coefficients obtained from the surrogates); 4. Reconstruction of the time-domain signal using the inverse MODWT and the cleaned coefficients. All the calculations were implemented in MATLAB (version R2019a, MathWorks Inc., Natick, MA, USA).

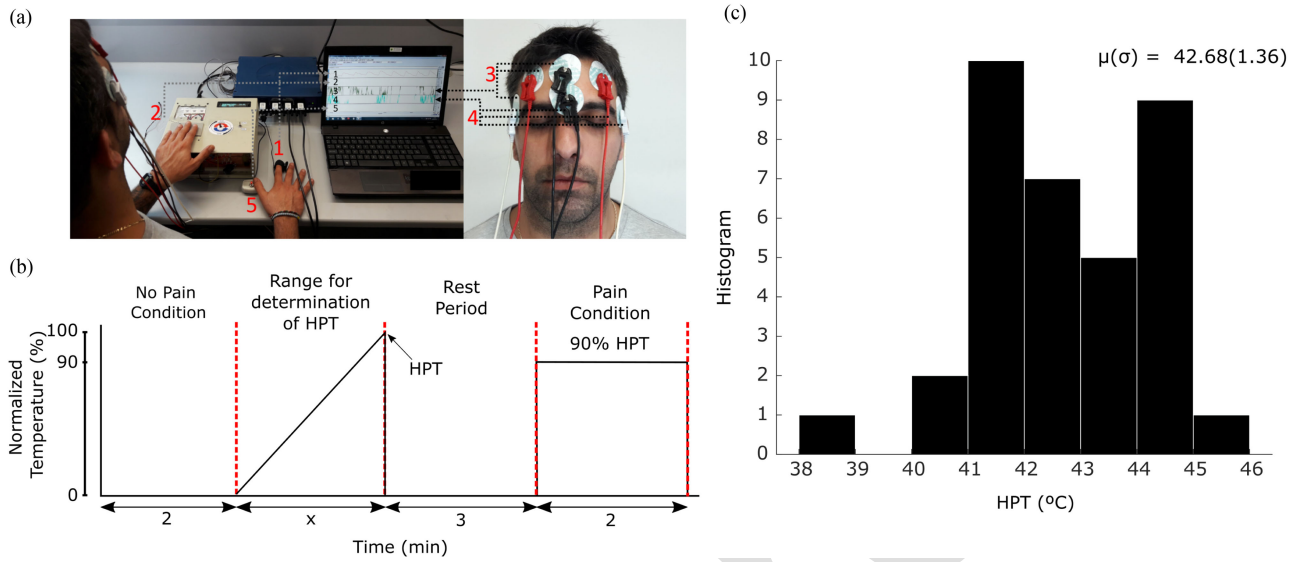

Fig. 1. **Device for pain perception studies. a**: System for the capture and recording of physiological signals. The PPG sensor (1) is attached to the distal phalanx of the index finger of the subject's hand, while the opposite hand is placed on the Peltier cell (2). The electrodes for the EEG signals (3,4) are placed on both sides of the forehead. Finally, the push-button is used to determine the thermoalgesic threshold. **b**: Pain stimulation is divided into four distinct regions, the first lasts 2 min in the absence of any painful stimulation to define the no pain condition. The second focuses on calculating the heat pain threshold (HPT) of x min, which was different for each participant. This phase was achieved by increasing the temperature in increments of 0.5 °C up to the HPT, the maximum temperature that the subject withstood. After a rest period of 3 min, a final regime to define the pain condition was achieved at the temperature equivalent to 90% of the HPT, lasting for 2 min. **c**: HPT histogram of all the participants, indicating the mean μ and standard deviation σ.

D. Stimulation Protocol

The system for data capture is shown in Fig. 1(a). There are two main elements to this set-up, the BioPac and the equipment to generate the stimulus connected to a portable unit. The Acq-Knowledge program displays the signals received from the PPG sensor (1), the sensor temperature (2) and the EEG (3,4), as well as the reference points inserted by a push-button to mark the point the heat pain threshold is reached (5), the maximum temperature that the subject can withstand in terms of exposure to heat pain. The no-pain condition (control) was obtained in complete absence of a painful stimulation (Fig. 1(b)), measuring the electrophysiological signals while keeping the participant's hand off the Peltier cell. This condition persisted for two minutes.

Signals were recorded over another two or three minutes to estimate the heat pain threshold (HPT) [24]. This was calculated while the participant placed one hand on the Peltier cell, recording the variables using the BioPac and progressively increasing the cell's temperature in a controlled fashion, varying it in increments of 0.5 °C up to the maximum temperature that the participant withstood, the HPT. This value was subject-dependent. The strategy of progressively increasing the temperature was critical in these experiments and it was performed in this way to achieve dual activation of the C receptors responsible for heat sensing and the Aδ fiber receptors that process noxious stimuli [25], [26].

A 2 minute recording was obtained during the pain stimulus, defined at a temperature equal to 90% of the HPT and chosen in this way as the maximum as possible without exceeding the Ethical Committee's recommendations. All the temperature values were transformed to values relative to the HPT and this normalization permits a comparative analysis across subjects.

Our study only included one experiment per subject.

E. Spectral Entropy to Detect Pain Perception

The SE is a generalization of the Shannon entropy, where the state probability $p(x)$ is replaced by a normalized power spectral density $p(f)$, which represents the probability density function of the power as a function of frequency. Here, the power SE was calculated through the absolute square of the Fast Fourier Transformation, calculated with the function *fft* in MATLAB. After normalization, we obtained $p(f)$ and from there, the one-dimensional spectral entropy was calculated as:

$$\mathrm{SE1} = -\sum_{f} p(f) \log p(f), \tag{1}$$

and applied individually to the three signals: EEG1 (left hemisphere), EEG2 (right hemisphere), and PPG.

For the two-dimensional SE we made use of the two-dimensional Fast Fourier *fft2* transformation in MATLAB, and after normalization, we defined:

$$\mathrm{SE2} = -\sum_{f_1} \sum_{f_2} p(f_1, f_2) \log p(f_1, f_2), \tag{2}$$

applied to any pairs of variables in the triplet EEG1, EEG2 and PPG.

Here, both SE1 and SE2 were calculated in 80%-of-overlapping windows of 5 Hz, and the code can be downloaded at https://github.com/compneurobilbao/spectral-entropy-maider.

Our choice of spectral entropy is motivated by the fact that different brain functions such as attention, memory consolidation, sleep, sensory processing, are well known to occur at specific EEG frequency bands. Here, for comparison purposes, we also made use of two well known time-domain entropies [27]–[30], such as Permutation Entropy and Multiscale Sample Entropy.

F. Statistical Analyses

For both SE1 and SE2, we calculated the FFT using the Blackman window function (implemented as *blackman* in Matlab) over time windows of 500 time points, and with a sampling frequency of 500 Hz, corresponding to 1 sec. After sliding the time window, we obtained a time series for SE1 and SE2, the latter representing a temporal sequence of the SE2 matrices. For each frequency value, the final SE1 and SE2 values were obtained by averaging all the entropy values in the temporal dimension. These temporal mean values of SE1 and SE2 were those used for the statistical comparison between the pain and no-pain conditions.

The discriminability between conditions was calculated as $\mathcal{D} \equiv \log_{10}(\text{pvalue})$, following the next four stages: We first calculated the SE1 and SE2 time series for each condition and subject, and we then averaged the two metrics over the entire time dimension. We then employed a Wilcoxon signed-rank test between the conditions, with the different subject measures considered as observations. This non-parametric test chosen for the comparison is valid for the case of non-Gaussian distributed data. Finally, to correct for multiple comparisons we applied a false-discovery-rate (FDR) and Bonferroni corrections, the latter using a significance threshold equal to $p^* = \frac{0.05}{\mathcal{F}}$, where $\mathcal{F}$ corresponds to the number of different frequencies used to compare the SE values (40 EEG and 10 for PPG). All the statistical analyses were performed in MATLAB (version R2019a, MathWorks Inc., Natick, MA, USA).

III. Results

A cohort of N = 35 subjects participated in the study. We obtained a HPT value for each subject when stimulated with our device (Fig. 1(c)), with a mean HPT of 42.68 °C (SD 1.36). For individual HPT values see Table I. There were apparently no significant gender differences in the HPT, as witnessed when the HPT of a subgroup of males (N=15, mean age 30.04 years: t-test = −0.46, p-value = 0.64) was compared with an age matched group of females (N = 15, mean age 29.23 years: t-test = −0.45, p-value = 0.63). This result was consistent with previous studies showing no differences over an age range similar to ours [31]. Importantly, normalization of the temperature values to the HPT allowed the two conditions of pain and no-pain to be defined independently of the participant, making the different metrics across participants and conditions comparable.

The SE values obtained from the different physiological signals between the pain and no-pain conditions were compared following the procedure explained in Fig. 2.

The statistical significance of all the possible comparisons was assessed with the discriminability (D) obtained from the p-values after a Wilcoxon signed-rank test was performed on the data from the different conditions (Methods, the discriminability is illustrated in Fig. 3(a) for the 1D case). Initially, the SE1 time series was calculated for each condition and participant, and the temporal averages were then calculated. These values were compared between conditions and across the different subjects (Fig. 3(a)), representing the value of D as a function of the different frequencies over which the comparisons were performed, i.e.: in the range of 1 to 40 Hz for the EEG and 1 to 10 Hz for the PPG.

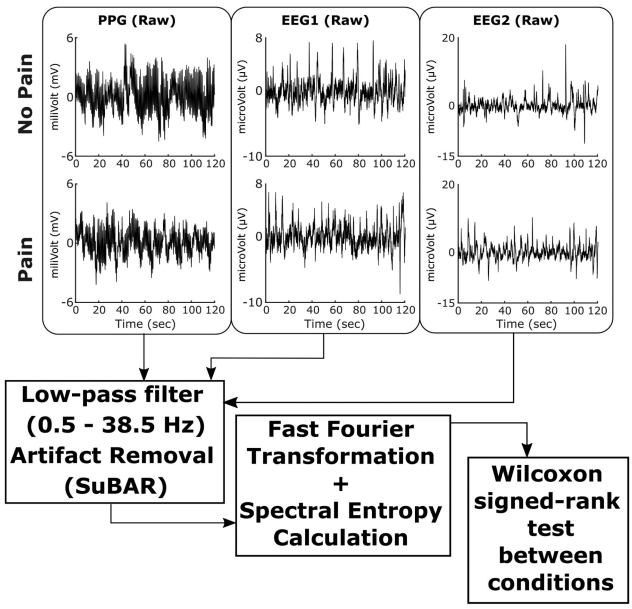

Fig. 2. **Signal processing workflow and statistical analysis.** For the analysis, we first separated the signals belonging to the different conditions, pain or no pain, applying a band-pass filter and artifact removal to each signal. The *fft* MATLAB function was then used to calculate the power spectrum, which was used to assess the spectral entropy (SE) at different frequency bands and with frequency windows of 5 Hz. Finally, we compared the SE across different conditions over different frequency ranges and across different participants.

As explained in the methods, SE1 was calculated within a window of size 5 Hz for each frequency value on the x-axis. Thus, the entropy was calculated in the range from 1 to 6 Hz for the value of 1 Hz on the x-axis, and in the range from 2 to 7 Hz for the value of 2, etc. Because the EEG and the PPG had different upper limits along the x-axis, the Bonferroni significance threshold also differed for the two modalities, as $\mathcal{F}$ was equal to 40 for the EEG and 10 for the PPG.

SE1 was able to discriminate the pain condition for the three sets of sensory data, EEG1 (purple line), EEG2 (yellow line) and PPG (green line), with the major discriminability found at 25–30 Hz for the EEG and at 5–10 Hz for the PPG (the region of Bonferroni significance is illustrated in Fig. 3(a) with a transparent dark-gray rectangle, while that for FDR correction is marked in light-gray). The evolution of SE1 over time was obtained from the three signals during 20 sec, which corresponded to 10000 time points for a sampling frequency of 500 HZ (Fig. 3(b)). After taking the temporal average of SE1, the mean entropy

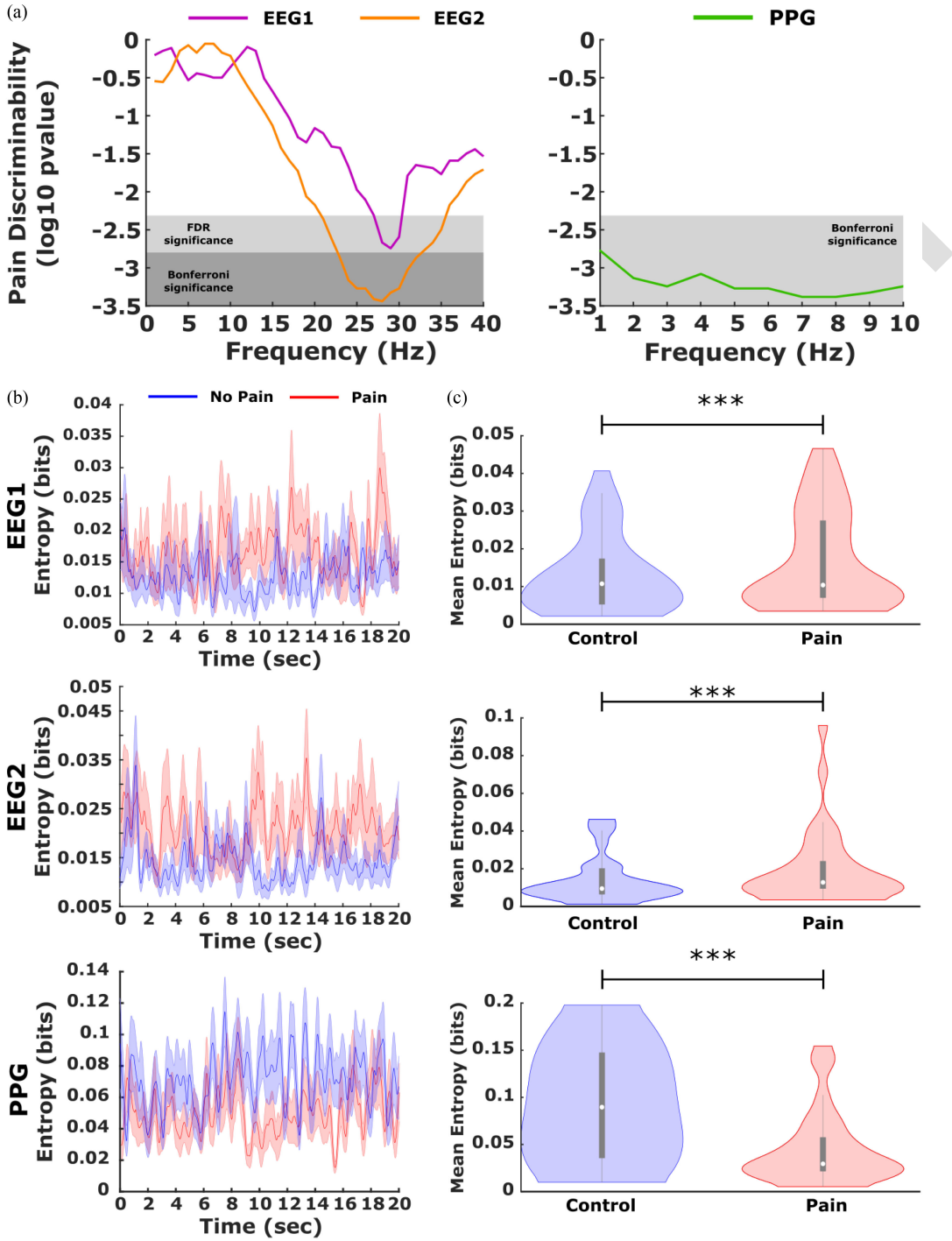

Fig. 3. **Discriminability of painful stimulation by 1D spectral entropy. a**: Discriminability $\mathcal{D} \equiv \log_{10}(\text{pvalue})$ as a function of the different frequencies over which the conditions were compared for values of SE1 using a Wilcoxon signed-rank test (Methods). For each signal and condition, SE1 was calculated over the entire time series. The temporal average was then taken and the resulting mean values of SE1 compared between the two conditions. Frequencies range from 1 to 40 Hz for the EEG and from 1 to 10 Hz for the PPG. For each frequency value on the x-axis, SE1 was calculated within a window of 5 Hz. Thus, for the value of 1 Hz in the x-axis, entropy was calculated in the range 1-6 Hz and similarly, for a value of 2 Hz it is in the range from 2-7 Hz. The FDR region and Bonferroni correction significance is marked by light and dark gray rectangles, respectively. **b**: SE1 as a function of time for fixed frequency values (29 Hz for EEG1, 28 Hz for EEG2 and 7 Hz for PPG) over a time interval of 20 sec. **c**: After averaging the temporal signal of SE1 (illustrated in panel B), comparing the conditions highlighted significant differences between pain and no pain for all signals. The gray rectangles within the violins represent the first and third quartiles, and the white dot within those rectangles represents the median of the distributions: *** indicates $p < 0.005$.

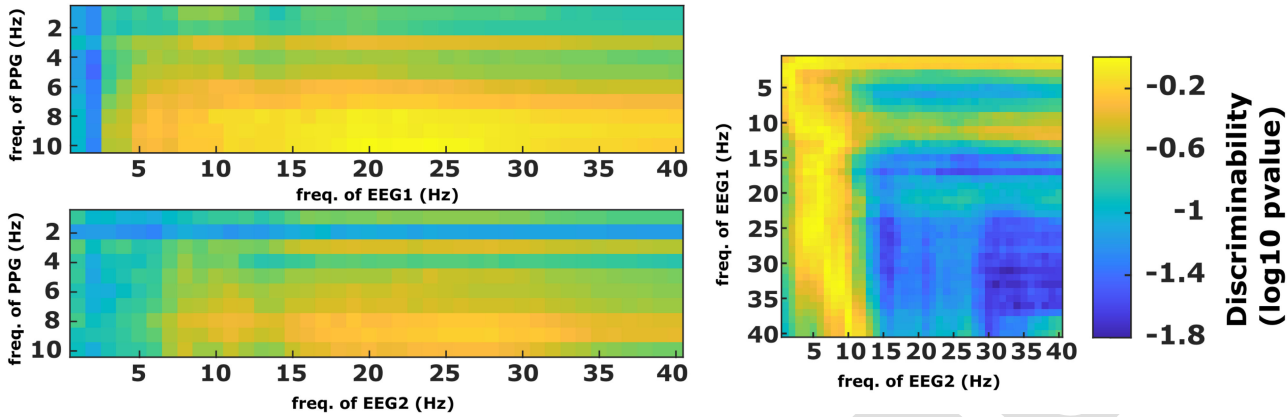

Fig. 4. **Discriminability of painful stimulation by 2D spectral entropy.** A similar strategy was followed to the SE1 strategy (Fig. 3) but now calculating the 2D spectral entropy (SE2). After comparing the values of the temporal mean of SE2 matrix entries using a Wilcoxon signed-rank test for different conditions (pain vs no pain). The surfaces of discriminability achieved by pairs of different signals (EEG1, EEG2), (EEG1, PPG) and (EEG2, PPG) were represented across different frequency ranges. Similar to SE1, SE2 was also calculated in squared windows of 5×5 Hz^2. The abbreviation freq. in the axis labels indicates frequency.

across participants provided significant differences between the conditions, as illustrated in Fig. 3(c). The values of maximum discriminability of SE1 for the three classes of signals EEG1, EEG2 and PPG were achieved at 29 Hz ($p < 10^{-2}$), 28 Hz ($p < 10^{-3}$) and 7 Hz ($p < 10^{-3}$), respectively.

The frequency band filtering of the signal for the discrimination of the painful vs the control stimulation was striking. When assessing discrimination using time-domain entropies with no filtered signals, neither the Permutation Entropy or the Multiscale Sample Entropy provided significant condition differences. However, when calculating these time-domain metrics to the windowed filter signal both the EEG and PPG did find significant differences (EEG1, freq. in 25-30 Hz, $p = 0.036$; PPG, freq. in 1–10 Hz, $p = 0.001$).

We also assessed the discriminability between the conditions that achieved SE2, analyzing the 2D SE values at different frequencies for the pairs of signals (EEG1, EEG2), (EEG1, PPG) and (EEG2, PPG), as well as across different frequency ranges (Fig. 4). Like SE1, SE2 was also calculated in squared windows of size 5 × 5 Hz^2. None of the comparisons of SE2 survived the Bonferroni correction or the FDR and thus, we only report here the uncorrected p-values. The values of maximum discriminability and the associated p-values occurred at (2,5) Hz for (PPG, EEG1: $p < 10^{-2}$) and at (33,31) Hz for (EEG1, EEG2: $p \approx 0.01$), yet they were not significant for PPG,EEG2 ($p = 0.05$).

IV. Discussion

Pain perception is a prototypic example of a well-orchestrated systemic response. Here, we have developed a compact device to simultaneously record physiological brain and heart parameters in response to a well-controlled painful thermal stimulus. The device consists of a Peltier cell that allows the temperature to be precisely varied under the control of an external computer, two EEG frontal electrodes (attached to the left and right hemispheres) and a PPG sensor located on one finger of the opposite hand to that on which the Peltier cell is placed. This platform can provide very precise information on the thresholds of maximum thermal tolerance to heat, which can potentially serve to assess novel strategies for both the diagnosis and follow-up of different pathological conditions.

Several studies have assessed the brain's response to heat induced pain using EEG [32]–[34], yet the novelty of this study is that a compact set-up has been developed to record the physiological responses of the heart and the brain while a subject receives a painful heat stimulus. This device enabled the mean heat pain threshold to be assessed in the cohort, defining a threshold of 42.68 °C in a population with a mean age of 30-years-old. This result was consistent with previous studies using quantitative sensory testing (QST) [24], [31], thereby validating the reliability of our device to measure heat pain thresholds.

Differences in pain perception between right and left hands were assessed before [35], [36]. In our cohort, we heated the right hand in 23 subjects and the left hand in the remaining 12 participants. For details see Table I. Our data did not show differences between left vs right heated hands (t-test = 1.58, p-value = 0.129). Furthermore, it is important to note that these values were obtained when heating one of the subject's hands for the first time. When we repeated the same procedure a second time on the contralateral hand soon after heating the first hand, the physiological response of the PPG differed from that reported here (data not shown). Hence, heating one hand affected the physiological response of the subsequent heating of the contralateral hand. Accordingly, further studies will be needed to fully clarify these relationships as here we focused on signals from the initial heating of one of the hands.

Our study shows that thermal pain is characterized by a reduction in the entropy of the heart response measured by PPG, which suggests that in addition to the autonomic nervous system's response, exposure to a thermal pain stimulus decreases the unpredictability of physiological systems as measured by their SE. In agreement with previous studies, we propose that

upper supraspinal centers might fulfil a critical role in this physiological process [37]. Moreover, the posterior ventral nucleus of the thalamus might also coordinate the visceral sensitivity as it is activated by mechanical and thermal stimuli in a nociceptive range [38]. Furthermore, we suggest that the primary and the secondary somatosensorial cortex, in addition to the Anterior Cingulate Cortex might be involved in this physiological mechanism [39], [40].

The novelty of our pain perception biomarkers relies on a combination of different aspects: a physiological response of the brain measured by the EEG while simultaneously recording the hemodynamics measured by the PPG. Moreover, we have exposed the subjects to a well control varying thermal stimulus using a new setup that allows the discrimination of pain vs control conditions within a specific range of frequencies. As far as we know previous studies incorporating all these ingredients have not been reported yet.

Other algorithms based on SE in different frequency bands have been introduced to monitor physiological states. The most widely known is the bispectral index (BIS), which is used in daily clinical practice to monitor the depth of anesthesia during surgical interventions in real-time [41], [42]. Through a device that uses four EEG electrodes located on the patient's forehead to measure the brain's electrical activity, BIS calculates the SEs in different frequency bands and combines them using a proprietary algorithm to produce a numeric index between 100 (no anesthesia) and 0 (maximum anesthesia, where the level of consciousness measured by the frontal EEG activity is zero). The FDA have validated that BIS levels between 40 and 60 are adequate for general anesthesia during surgical interventions. For pain perception, such FDA-approved indices do not exist to date.

It is well-known that several chronic pain syndromes are associated with alterations to the activity of the Descending Nociceptive Inhibitory System (DNIS), such as fibromyalgia, painful diabetic neuropathy and lower back pain [43]–[45]. The DNIS is comprised of a network of cortical and subcortical brain areas, including the anterior insula, middle frontal gyri and amygdala, and the rostral ventromedial medulla and periaqueductal gray brainstem regions, which can inhibit nociceptive afferent brain input [46], [47]. A relationship between the DNIS and Heart Rate Variability (HRV) has been shown, whereby patients with an impaired DNIS have a lower resting HRV [48], consistent with the reduced entropy found here [49], [50]. Moreover, an abnormally low HRV was detected in a group of individuals with Chronic Fatigue Syndrome, indicating that they might have weaker parasympathetic modulation of their heart rate [51]. In other chronic pain syndromes like fibromyalgia, a reduced HRV was thought to reflect weaker emotional adaptability and resistance to stress [52].

Our findings reveal a close relationship between pain perception and the brain's physiological entropy at different frequencies, in agreement with previous studies showing that pain is associated with a spatially extended network of dynamically recruited brain areas, resulting in complex temporal–spectral patterns of brain activity [53]. In particular, pain produces individual variations in the SE of both EEG and PPG at different frequencies (measured by SE1), as well as in their bi-dimensional interaction (as by SE2). Pain-related neuronal oscillations were observed previously at Theta (4–7 Hz), Alpha (8–13 Hz), Beta (14–29 Hz), and Gamma (30–200 Hz) frequencies [54]–[57]. Here, we found that both left-hemisphere EEG and right-hemisphere EEG have the best discrimination of the painful stimulus in the Beta and Theta band, and then in the Alpha and Gamma bands, as seen elsewhere [53], [54], [58].

Our work is a first step advancing in the manufacturing and analyses of systemic response to thermoalgesic stimulation, but it has also some limitations. First, although we tried to keep the volunteers calm by playing relaxing music while recording the physiological response to the thermoalgesic stimulus, we did not control the arousal, attention or salience, nor did we assessed cognitive appraisal before or during the experiment. Second, we focused this study on thermoalgesic stimulation, yet different painful stimuli could be incorporated into our device for future studies, for instance mechanical pain, providing greater sensitivity and specificity to discriminate different classes of painful stimulation. Third, different to what is typically performed in EEG experiments where multiple stimulus-response trials are recorded, we did not repeat painful stimulation to the same subjects hand, as the physiological adaptation or conditioning of the nerve fibers might change the results. Future studies assessing the repeatability of painful stimuli are needed for further understanding of these complex interactions. Fourth, the temperature of the Peltier cell was varied in increments of 0.5 °C to achieve the activation of C receptors (responsible for heat processing) together with that of the Aδ fiber receptors (responsible for noxious processing stimuli) [25], [26], a critical constraint to our design. Moreover, we did not assess systematic variations in the increasing temperature intervals, but future studies should also explore different protocols for increasing temperature. Fifth, our protocol did not allow the thermoalgesic exposure to heat to be randomized, which could possibly be incorporated into the stimulation protocol in future studies. Finally, the young adult healthy population recruited here did not show differences between left and right hands. However, whether significant differences might exist in some pathological conditions is intriguing and should be clarified elsewhere, as this is beyond the scope of the present work.

In summary, our compact device allows brain and heart physiological signals to be recorded simultaneously in response to well-controlled thermal pain stimuli. We show that the SE of the physiological signals can discriminate pain states. Future work should validate similar metrics based on SE for the on-line variation of painful stimuli, or the dynamic on-line interaction between PPG and EEG signals, for instance using Granger causality [59]–[62] or transfer entropy [63], [64], as used previously to establish different dynamic brain mechanisms in pain-related conditions like migraine [65], [66]. Last but not least, future studies should assess whether our dual EEG and PPG system is useful to study some pathological conditions in which the autonomic nervous system functions abnormally, such as small fiber neuropathies, fibromyalgia or painful diabetic neuropathy.

ACKNOWLEDGMENT

We acknowledge the assistance of Javier Rasero through critical reading of this manuscript and his constructive suggestions for the statistical analysis.

AUTHOR CONTRIBUTIONS

Manufacturing of the hardware device: MNI, JOAC; Patient recruitment: MNI; Design and implementation of the signal processing methods: BCP, ID, AE, JMC; Figure preparation: MNI, BCP, JMC; Draft of the manuscript: MNI, BCP, ID, AE, EMG, SS, JOAC, JMC; Supervision of the research - equal contribution: JOAC, JMC;

REFERENCES

[1] L. A. Jorgenson *et al.*, "The BRAIN initiative: Developing technology to catalyse neuroscience discovery," *Philos. Trans. Roy. Soc. London B. Biol. Sci.*, vol. 370, 2015, Art. no. 20140164.

[2] A. M. Carek and O. T. Inan, "A temperature-controlled glove with non-invasive arterial pulse sensing for active neuro-vascular assessment," in *Proc. 38th IEEE Annu. Int. Conf. Eng. Med. Biol. Soc.*. Orlando, FL, USA, Aug. 2016, pp. 619–622.

[3] D. Ward, N. Z. Gurel, O. T. Inan, and F. L. Hammond, "A soft thermal modulation and physiological sensing system for neuro-vascular assessment," in *Proc. IEEE Int. Conf. Robot. Biomimetics*. Kuala Lumpur, Malaysia, Dec. 2018, pp. 991–998.

[4] N. Z. Gurel, D. Ward, F. L. Hammond, and O. T. Inan, "Live demonstration: A soft thermal modulation system with embedded fluid channels for neuro-vascular assessment," in *Proc. IEEE Biomed. Circuits Syst. Conf.*. Cleveland, OH, Oct. 2018, pp. 1–1.

Q3 [5] A. Bashan, R. P. Bartsch, J. W. Kantelhardt, S. Havlin, and P. C. Ivanov, "Network physiology reveals relations between network topology and physiological function," *Nature Commun.*, vol. 3, p. 702, 2012.

[6] R. P. Bartsch, K. K. L. Liu, A. Bashan, and P. C. Ivanov, "Network physiology: How organ systems dynamically interact," *PLoS One*, vol. 10, 2015, Art. no. e0142143.

[7] P. Ivanov, X. Zhang, and F. Lombardi, "The new field of network physiology: Mapping the human physiolome," *APS Mar. Meeting Abstracts*, vol. 2019, 2019, Art. no. A56.004.

[8] H. Merskey, "An investigation of pain in psychological illness," Ph.D. dissertation, Univ. Oxford, 1964.

Q4 [9] E. Gentile, A. Brunetti, K. Ricci, M. Delussi, V. Bevilacqua, and M. de Tommaso, "Mutual interaction between motor cortex activation and pain in fibromyalgia: EEG-fNIRS study," *PLoS One*, vol. 15, no. 1, Jan. 2020, Art. no. e0228158.

[10] E. Gentile, K. Ricci, M. Delussi, and M. de Tommaso, "Motor cortex function in fibromyalgia: A pilot study involving near-infrared spectroscopy and co-recording of laser-evoked potentials," *Funct. Neurol.*, vol. 34, no. 2, pp. 107–118, Jun. 2019.

[11] S. Koyama *et al.*, "An electroencephalography bioassay for preclinical testing of analgesic efficacy," *Sci. Rep.*, vol. 8, 2018, Art. no. 16402.

[12] E. R. J. Seitsonen *et al.*, "EEG spectral entropy, heart rate, photoplethysmography and motor responses to skin incision during sevoflurane anaesthesia," *Acta Anaesthesiol. Scand.*, vol. 49, pp. 284–292, 2005.

[13] M. de Tommaso, "An update on EEG in migraine," *Expert Rev. Neurotherapeutics*, vol. 19, no. 8, pp. 729–737, Aug. 2019.

[14] H. Lim, B. Kim, G. J. Noh, and S. Yoo, "A deep neural network-based pain classifier using a photoplethysmography signal," *Sensors*, vol. 19, p. 384, 2019.

[15] K. Hamunen, V. Kontinen, E. Hakala, P. Talke, M. Paloheimo, and E. Kalso, "Effect of pain on autonomic nervous system indices derived from photoplethysmography in healthy volunteers," *Brit. J. Anaesth.*, vol. 108, pp. 838–844, 2012.

[16] H. Fruhstorfer, W. Gross, and O. Selbmann, "Von Frey hairs: New materials for a new design," *Eur. J. Pain*, vol. 5, pp. 341–342, 2001.

[17] S. Cathcart and D. Pritchard, "Reliability of pain threshold measurement in young adults," *J. Headache Pain*, vol. 7, pp. 21–26, 2006.

[18] M. Huiku *et al.*, "Assessment of surgical stress during general anaesthesia," *Brit. J. Anaesth.*, vol. 98, pp. 447–455, 2007.

[19] E. Castrillon *et al.*, "Entropy of masseter muscle pain sensitivity: A new technique for pain assessment," *J. Oral Facial Pain Headache*, vol. 31, pp. 87–94, 2017.

[20] J. N. Acharya, A. Hani, J. Cheek, P. Thirumala, and T. M. Tsuchida, "American clinical neurophysiology society guideline 2: Guidelines for standard electrode position nomenclature," *J. Clin. Neurophysiol.*, vol. 33, pp. 308–311, 2016.

[21] G. Perlaki *et al.*, "Pain-related autonomic response is modulated by the medial prefrontal cortex: An ECG-fMRI study in men," *J. Neurol. Sci.*, vol. 349, pp. 202–208, 2015.

[22] S. Lu *et al.*, "Can photoplethysmography variability serve as an alternative approach to obtain heart rate variability information?," *J. Clin. Monit. Comput.*, vol. 22, pp. 23–29, 2008.

[23] M. Chavez, F. Grosselin, A. Bussalb, F. D. V. Fallani, and X. Navarro-Sune, "Surrogate-based artifact removal from single-channel EEG," *IEEE Trans. Neural Syst. Rehabil. Eng.*, vol. 26, no. 3, pp. 540–550, Mar. 2018.

[24] R. Rolke *et al.*, "Quantitative sensory testing: A comprehensive protocol for clinical trials," *Eur. J. Pain*, vol. 10, p. 77, 2006.

[25] A. Cervera, M. Veciana, and J. Valls-Sole, "Sympathetic sudomotor skin responses induced by laser stimuli in normal human subjects," *Neurosci. Lett.*, vol. 334, pp. 115–118, 2002.

[26] L. Plaghki and A. Mouraux, "How do we selectively activate skin nociceptors with a high power infrared laser? Physiology and biophysics of laser stimulation," *Neurophysiol. Clin.*, vol. 33, pp. 269–277, 2003.

[27] C.-W. Woo *et al.*, "Quantifying cerebral contributions to pain beyond nociception," *Nature Commun.*, vol. 8, no. 1, Apr. 2017, Art. no. 14211.

[28] N. Mammone, C. Ieracitano, H. Adeli, A. Bramanti, and F. C. Morabito, "Permutation jaccard distance-based hierarchical clustering to estimate EEG network density modifications in MCI subjects," *IEEE Trans. Neural Netw. Learn. Syst.*, vol. 29, no. 10, pp. 5122–5135, Oct. 2018.

[29] X. Li, G. Ouyang, and D. A. Richards, "Predictability analysis of absence seizures with permutation entropy," *Epilepsy Res.*, vol. 77, no. 1, pp. 70–74, Oct. 2007.

[30] M. Costa, A. L. Goldberger, and C.-K. Peng, "Multiscale entropy analysis of biological signals," *Phys. Rev. E*, vol. 71, no. 2, Feb. 2005, Art. no. 021906.

[31] W. Magerl, E. K. Krumovab, R. Baron, T. Tolle, R. D. Treede, and C. Maier, "Reference data for quantitative sensory testing (QST): Refined stratification for age and a novel method for statistical comparison of group data," *Pain*, vol. 151, pp. 598–605, 2010.

[32] G. Liberati, M. Algoet, S. F. Santos, J. G. Ribeiro-Vaz, C. Raftopoulos, and A. Mouraux, "Tonic thermonociceptive stimulation selectively modulates ongoing neural oscillations in the human posterior insula: Evidence from intracerebral EEG," *NeuroImage*, vol. 188, pp. 70–83, 2019.

[33] E. Colon, V. Legrain, and A. Mouraux, "EEG frequency tagging to dissociate the cortical responses to nociceptive and nonnociceptive stimuli," *J. Cogn. Neurosci.*, vol. 26, pp. 2262–2274, 2014.

[34] J. H. Kim, J. H. Chien, C. C. Liu, and F. A. Lenz, "Painful cutaneous laser stimuli induce event-related gamma-band activity in the lateral thalamus of humans," *J. Neurophysiol.*, vol. 113, pp. 1564–1573, 2015.

[35] A. Eken, M. Kara, B. Baskak, A. Baltacı, and D. Gökçay, "Differential efficiency of transcutaneous electrical nerve stimulation in dominant versus nondominant hands in fibromyalgia: Placebo-controlled functional near-infrared spectroscopy study," *Neurophotonics*, vol. 5, no. 1, p. 1, Sep. 2017.

[36] D. Pud, Y. Golan, and R. Pesta, "Hand dominancy-a feature affecting sensitivity to pain," *Neurosci. Lett.*, vol. 467, no. 3, pp. 237–240, Dec. 2009.

[37] M. J. Millan, "Descending control of pain," *Prog. Neurobiol.*, vol. 66, pp. 355–474, 2002.

[38] A. May, "Chronic pain may change the structure of the brain," *Pain*, vol. 137, pp. 7–15, 2008.

[39] J. A. García-Porrero Pérez, L. Ezquerra Polo, il, and J. M. Hurlé, *Neuroanatomía Humana*. Editorial Medica Panamericana, 2015.

[40] A. Mouraux and G. D. Iannetti, "The search for pain biomarkers in the human brain," *Brain*, vol. 141, pp. 3290–3307, 2018.

[41] P. S. Myles, K. Leslie, J. McNeil, A. Forbes, and M. T. Chan, "Bispectral index monitoring to prevent awareness during anaesthesia: The B-aware randomised controlled trial," *Lancet*, vol. 363, no. 9423, pp. 1757–1763, 2004.

[42] S. S. Liu, "Effects of bispectral index monitoring on ambulatory anesthesia: A meta-analysis of randomized controlled trials and a cost analysis," *Anesthesiology*, vol. 101, pp. 311–315, 2004.

[43] A. P. Brietzke *et al.*, "Potency of descending pain modulatory system is linked with peripheral sensory dysfunction in fibromyalgia: An exploratory study," *Medicine*, vol. 98, 2019, Art. no. e13477.

[44] J. T. Kong *et al.*, "Central mechanisms of real and sham electroacupuncture in the treatment of chronic low back pain: Study protocol for a randomized, placebo-controlled clinical trial," *Trials*, vol. 19, p. 685, 2018.
[45] A. R. Segerdahl, A. C. Themistocleous, D. Fido, D. L. Bennett, and I. Tracey, "A brain-based pain facilitation mechanism contributes to painful diabetic polyneuropathy," *Brain*, vol. 141, pp. 357–364, 2018.
[46] M. H. Ossipov, G. O. Dussor, and F. Porreca, "Central modulation of pain," *J. Clin. Investig.*, vol. 120, pp. 3779–3787, 2010.
[47] P. Schweinhardt and M. C. Bushnell, "Pain imaging in health and disease - How far have we come?," *J. Clin. Investig.*, vol. 120, pp. 3788–3797, 2010.
[48] P. Rodrigues, L. Correa, M. Ribeiro, B. Silva, F. Reis, and L. Nogueira, "Patients with impaired descending nociceptive inhibitory system present altered cardiac vagal control at rest," *Pain Physician*, vol. 21, pp. E409–E418, 2018.
[49] J. S. Richman and J. R. Moorman, "Physiological time-series analysis using approximate entropy and sample entropy," *Amer. J. Physiol. Heart Circ. Physiol.*, vol. 278, pp. H2039–H2049, 2000.
[50] M. Costa, A. L. Goldberger, and C. K. Peng, "Multiscale entropy analysis of complex physiologic time series," *Phys. Rev. Lett.*, vol. 89, 2002, Art. no. 068102.
[51] K. A. Rimes, K. Lievesley, and T. Chalder, "Stress vulnerability in adolescents with chronic fatigue syndrome: Experimental study investigating heart rate variability and skin conductance responses," *J. Child. Psychol. Psychiatry*, vol. 58, pp. 851–858, 2017.
[52] M. Reneau, "Heart rate variability biofeedback to treat fibromyalgia: An integrative literature review," *Pain Manage. Nurs.*, 2019, Art. no. S1524904217306732.
[53] M. Ploner, C. Sorg, and J. Gross, "Brain rhythms of pain," *Trends Cogn. Sci.*, vol. 21, pp. 100–110, 2017.
[54] Y. Huang, H. Luo, A. L. Green, T. Z. Aziz, and S. Wang, "Characteristics of local field potentials correlate with pain relief by deep brain stimulation," *Clin. Neurophysiol.*, vol. 127, pp. 2573–2580, 2016.
[55] A. L. Green *et al.*, "Nueral signatures in patients with neuropathic pain," *Neurology*, vol. 72, pp. 569–571, 2009.
[56] M. N. Baliki, A. T. Baria, and A. V. Apkarian, "The cortical rhythms of chronic back pain," *J. Neurosci.*, vol. 31, pp. 13981–13990, 2011.
[57] Z. G. Zhang, L. Hu, Y. S. Hung, A. Mouraux, and G. D. Iannetti, "Gamma-band oscillations in the primary somatosensory cortex-a direct and obligatory correlate of subjective pain intensity," *J. Neurosci.*, vol. 32, pp. 7429–7438, 2012.
[58] K. D. Walton and R. R. Llinás, "Central pain as a thalamocortical dysrhythmia: A thalamic efference disconnection?" in *Translational Pain Research: From Mouse to Man*, L. Kruger and A. R. Light, Eds. CRC Press/Taylor & Francis, 2010.
[59] D. Marinazzo, M. Pellicoro, and S. Stramaglia, "Kernel method for nonlinear granger causality," *Phys. Rev. Lett.*, vol. 100, 2008, Art. no. 144103.
[60] L. Faes, G. Nollo, S. Stramaglia, and D. Marinazzo, "Multiscale granger causality," *Phys. Rev. E*, vol. 96, 2008, Art. no. 144103.
[61] S. Stramaglia, L. Angelini, G. Wu, J. M. Cortes, L. Faes, and D. Marinazzo, "Synergetic and redundant information flow detected by unnormalized granger causality: Application to resting state fMRI," *IEEE Trans. Biomed. Eng.*, vol. 63, no. 12, pp. 2518–2524, Dec. 2016.
[62] C. Alonso-Montes *et al.*, "Lagged and instantaneous dynamical influences related to brain structural connectivity," *Front. Psychol.*, vol. 6, 2015, Art. no. 1024.
[63] A. Erramuzpe *et al.*, "Identification of redundant and synergetic circuits in triplets of electrophysiological data," *J. Neural Eng.*, vol. 12, 2015, Art. no. 066007.
[64] I. Diez *et al.*, "Information flow between resting-state networks," *Brain Connect*, vol. 5, pp. 554–564, 2015.
[65] M. Tommaso *et al.*, "Altered processing of sensory stimuli in patients with migraine," *Nature Rev. Neurol.*, vol. 10, pp. 144–155, 2014.
[66] M. Tommaso, G. Trotta, E. Vecchio, K. Ricci, R. Siugzdaite, and S. Stramaglia, "Brain networking analysis in migraine with and without aura," *J. Headache Pain*, vol. 18, p. 98, 2017.